Perspectives on field-free spin-orbit torque devices for memory and computing applications

Victor Lopez-Dominguez [1,2*], Yixin Shao [1,2], Pedram Khalili Amiri [1,2#]

[1] Department of Electrical and Computer Engineering, Northwestern University, Evanston, Illinois 60208, United States of America

[2] Physical Electronics Research Laboratory (PERL), Northwestern University, Evanston, Illinois 60208, United States of America

[*] Email: victor@northwestern.edu

[#] Email: pedram@northwestern.edu

Abstract

The emergence of embedded magnetic random-access memory (MRAM) and its integration in mainstream semiconductor manufacturing technology has created an unprecedented opportunity for engineering computing systems with improved performance, energy efficiency, lower cost, and unconventional computing capabilities. While the initial interest in the existing generation of MRAM – which is based on the spin-transfer torque (STT) effect in ferromagnetic tunnel junctions – was driven by its nonvolatile data retention and lower cost of integration compared to embedded Flash (eFlash), the focus of MRAM research and development efforts is increasingly shifting towards alternative write mechanisms (beyond STT) and new materials (beyond ferromagnets) in recent years. This has been driven by the need for better speed versus density and speed versus endurance tradeoffs, to make MRAM applicable to a wider range of memory markets, as well as to utilize the potential of MRAM in various unconventional computing architectures that utilize the physics of nanoscale magnets. In this Perspective, we offer an overview of spin-orbit torque (SOT) as one of these beyond-STT write mechanisms for MRAM devices. We discuss, specifically, the progress in developing SOT-MRAM devices with a perpendicular magnetization. Starting from basic symmetry considerations, we discuss the requirement for an in-plane bias magnetic field which has hindered progress in developing practical SOT-MRAM devices. We then discuss several approaches based on structural, magnetic, and chiral symmetry-breaking that have been explored to overcome this limitation and realize bias-field-free SOT-MRAM devices with perpendicular magnetization. We also review the corresponding material- and device-level challenges in each case. We then present a perspective of the potential of these devices for computing and security applications, beyond their use in the conventional memory hierarchy.

I. Introduction: The need for emerging memory technologies

Driven by increasingly data- and memory-intensive computing applications[1], and their corresponding energy consumption, performance, and cost challenges, the past decade has witnessed a significant interest in emerging memory technologies across the semiconductor industry[2-5]. These emerging devices have generally been targeted towards one of three goals:

a. Embedded memory (EM): Non-traditional EM candidates seek to either offer a higher-density version of static random-access memory (SRAM), to reduce the overall portion of the area occupied by SRAM in existing microprocessors, special-purpose (e.g., graphics or machine learning) processors, and other application-specific integrated circuits[6-9]; or offer a nonvolatile memory technology that can be integrated in existing advanced complementary metal-oxide-silicon (CMOS) logic manufacturing processes, without a significant added cost, for example to replace embedded Flash (eFlash) at CMOS nodes below 28 nm[10-13]. In some cases, these alternative EM candidates can achieve density (hence cost per bit) and speed that bridges SRAM and dynamic random-access memory (DRAM), as illustrated in Fig. 1. Much of the current activities on MRAM development fall within this category. The following discussion of SOT-MRAM development in this Perspective is also mostly, though not exclusively, focused on embedded applications.
b. Storage-class memory (SCM): SCM candidates are memory technologies whose performance and density falls within the (large) gap that exists between NAND Flash (i.e., storage) and DRAM (i.e., memory). It has been suggested that the existence of such a new intermediate tier can improve overall system performance and cost[14,15]. Several technologies including phase change[16], resistive[17], and magnetic memories have been explored as SCM[18]. A challenge with this approach has been the need for SCM to use existing DRAM or NAND interfaces for use in products, which somewhat limits the potential performance gains expected from the technology. The recent emergence of Compute Express Link (CXL)[19,20] may affect future research in this area, and may also help NAND and DRAM to address parts of the above-mentioned performance and cost gap, thus narrowing the opportunity for emerging memories.
c. Unconventional computing (UC): The adoption of new memory technologies within the semiconductor industry also provides unprecedented opportunities to use their unique physics in new ways to perform computing tasks that are traditionally difficult in CMOS technology. Examples of this include matrix multiplication using analog weights encoded in memristors[21-25], stochastic computing implementation of neural

networks to improve their size and energy efficiency[26-32], as well as reservoir, probabilistic, and other physics-based approaches to computing that utilize the physics of emerging nanodevices[33-36].

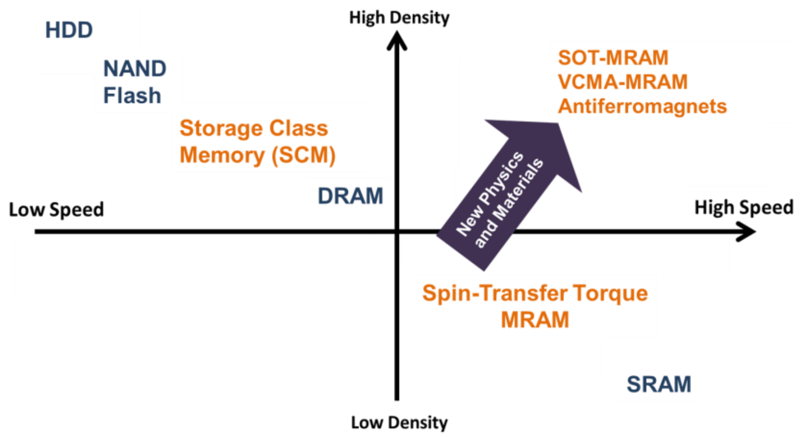

Fig. 1: Overview of the landscape of existing (dark blue) and emerging (orange) memory technologies, highlighting the fundamental tradeoff between bit density (loosely correlated with cost per bit) and speed. Emerging materials and physical mechanisms for MRAM, such as spin-orbit torque (SOT) and voltage-controlled magnetic anisotropy (VCMA), aim to achieve a better combination of speed and density than is possible with existing spin-transfer torque (STT) MRAM.

II. Basic properties of magnetic random-access memory

Magnetic random-access memory (MRAM) is the leading contender for EM applications due to its relative ease of integration (availability of 300 mm processing tools) within existing semiconductor processes, high endurance, speed, and nonvolatile data retention. MRAM utilizes a magnetic tunnel junction (MTJ) to store information (Fig. 2a), which consists of two ferromagnetic (FM) layers, separated by an insulating tunnel barrier. The tunneling resistance across this stack depends on the relative orientation (parallel, P or antiparallel, AP) of the two FM layers. Thus, by using a low-anisotropy FM material as the free layer and by using a number of established techniques to make the other FM layer harder to switch (i.e., fixed or pinned), one can create a memory device with a resistive readout using the tunneling magnetoresistance (TMR) effect[37-44]. Conventionally, currents passed directly through this trilayer transfer angular momentum to the free layer magnetization via the STT effect, thus resulting in switching of the magnetization with a preferred directionality that depends on the current direction[45-49]. This type of TMR read and STT write operation can be implemented by integrating a field-effect transistor (FET) in series with the MTJ, as shown in Fig. 2a, resulting in a compact one transistor - one resistor (1T-1R) memory cell architecture, somewhat resembling that of DRAM.

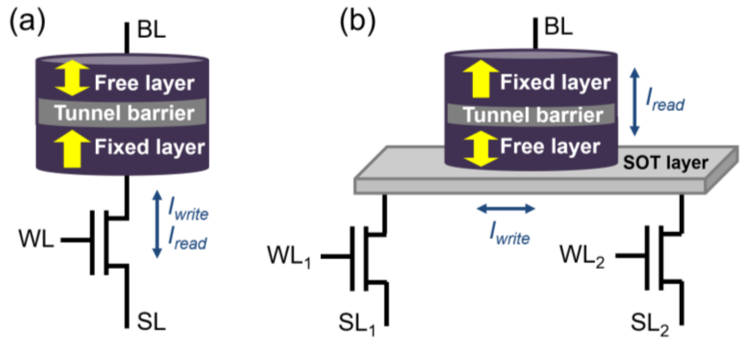

Fig. 2: Typical structure of (a) STT- and (b) SOT-MRAM cells, where the access transistor(s), bit line (BL), word line(s) (WL), and source line(s) (SL) are also shown. The three-terminal SOT structure separates the read and write paths, thus alleviating the endurance and read disturb issues of STT-MRAM, at the price of adding a third terminal and thus making the cell structure larger. More importantly, for a perpendicularly magnetized free layer, an additional in-plane symmetry-breaking mechanism is required to make the current-induced switching in (b) deterministic. This can be achieved by a number of methods including magnetic bias fields, as well as structural, magnetic and chiral symmetry-breaking methods.

III. Spin-orbit torque as an emerging write mechanism for MRAM

A different method of current-controlled switching of MTJs can be realized by placing a material with large spin-orbit coupling (SOC) – for example, a heavy metal or topological insulator – in direct contact with the MTJ free layer[50-57], as illustrated in Fig. 2b. In contrast to STT switching, where the passing of electrons through a ferromagnetic layer within the MTJ results in a net spin-polarized current, in SOT-controlled MTJs, it is the SOC – through the spin Hall or interfacial Rashba effects – that creates a net spin current which is perpendicular to the direction of charge current, and conventionally (although not always, as described later), also has a spin polarization that is perpendicular to both the charge and spin current directions[58].

The key reasons for the introduction of SOT as an emerging write mechanism for MRAM are twofold:

a. By taking advantage of the three-terminal device geometry to improve the current-induced switching efficiency (i.e., switching with a lower overall current) it can, in principle, lead to fast switching without necessitating the use of large access transistors, which is a significant challenge for STT-MRAM cells such as the one shown in Fig. 2a. This comes at the expense of adding a third terminal to the memory device which, in the most straightforward circuit implementation, necessitates the use of two transistors per SOT-MRAM memory cell, thus resulting in a two transistor - one resistor (2T-1R) memory cell (Fig. 2b). Recent works have, however, made advances in also demonstrating two-terminal SOT-MRAM operation by either using a combination of STT and SOT in the same device, or by using the nonuniform distribution of current within the SOC layer[59-62]. However, the scalability of these approaches to technologically relevant SOT-MRAM cell sizes remains to be demonstrated.
b. The separation of read and write paths in the three-terminal SOT-MRAM cell geometry eliminates the endurance issues that challenge two-terminal STT-MRAM cells, where the application of relatively large electric fields during the write operation across the MgO tunnel barrier (on the order of ~ 0.5 V/nm) results in its gradual deterioration and breakdown. This separation also allows the device designer additional flexibility to avoid disturbing the bit state during the read operation, which is a well-known challenge of conventional STT-MRAM cells.

IV. SOT-MRAM with perpendicular magnetization: Symmetry considerations

Despite the above advantages, SOT-MRAM faces a key challenge due to the difficulty of using conventional SOT effects to switch free layers with a perpendicular easy axis (i.e., out-of-plane magnetization). This follows from the symmetry of the SOT structure shown in Fig. 2b (which also has a perpendicularly magnetized free layer), as described below.

Out-of-plane magnetization of the free layer is desirable for scaled MRAM, due to the relative ease of lithographically patterning circular MTJs (as opposed to ellipses used for in-plane MRAM cells where shape anisotropy defines the free layer states), as well as the ability to achieve higher free layer energy barriers (i.e., data retention time) by taking advantage of bulk or interfacial perpendicular anisotropy[63-65]. However, in the conventional SOT-MRAM geometry (See Fig. 2b), there is no mechanism for in-plane currents to be directionally associated with a particular direction of the perpendicular magnetization (i.e., desired final state after switching), due to the in-plane symmetry of the structure. The conventional method to overcome this challenge is the application of an in-plane magnetic bias field[53,54,66], which breaks the in-plane symmetry of the device and therefore allows deterministic and directional SOT-induced switching to occur. This approach is illustrated in Fig. 3, following a symmetry analysis first described in Ref. 67.

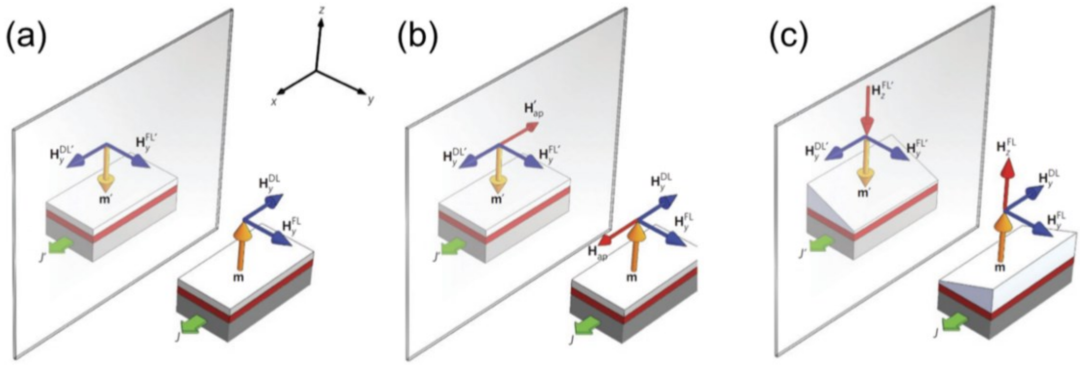

Fig. 3: Symmetry analysis of SOT switching of a perpendicular magnet using an in-plane electric current (Reproduced with permission from Ref. 67). (a) In a structure that is symmetric with respect to the *xz* plane (i.e., mirror), an in-plane current density vector J is not directionally associated with a preferred orientation of the magnetization m. The effective fields due to conventional damping-like (DL) and field-like (FL) torques are also shown. (b) An in-plane applied bias field (H_{ap}) breaks the in-plane symmetry, allowing for directional SOT-induced switching. (c) A broken in-plane structural symmetry (in this case, depicted as a laterally varying layer thickness within the device) can also result in directional and deterministic switching, without the need for a bias field.

This type of in-plane bias field can, in principle, be integrated into an MTJ for SOT-MRAM applications, as illustrated in a few works, for example by using the magnetic dipole coupling to an in-plane fixed ferromagnetic layer in close proximity to the free layer[68,69]. However, this is undesirable for at least three reasons: (i) The energy barrier between the two perpendicular free layer states is reduced as a result of the in-plane bias field, thus negating of the original reasons of using a perpendicular free layer in the device. (ii) The statistical distribution of this in-plane stray field can create an additional source of device-to-device variability in a memory chip, making it difficult to design a reliable product with uniform switching characteristics. (iii) The additional in-plane fixed layer will typically increase the overall thickness of the MTJ stack, which can make it more difficult to achieve tight pitch between neighboring MTJs in high-density memory arrays.

As a result, recent years have seen a wide range of methods being explored for the development of bias-field-free SOT-MRAM devices with an out-of-plane free layer magnetization. The following sections present three of these approaches, based on structural, magnetic, and chiral broken in-plane symmetry. It is worth noting that our intention here is not to present a comprehensive accounting of reports on bias-field-free SOT switching to date, but rather, to highlight some of the most illustrative examples that can highlight key challenges and possible directions for future research in this field.

V. Field-free SOT-MRAM based on structural asymmetry

A general approach to realizing field-free directional switching of out-of-plane magnetization is to break the in-plane symmetry of the SOT device using an element other than an applied field. The first approach to do so is to use broken in-plane *structural* symmetry, as illustrated in Fig. 3c. Note that the symmetry analysis of the type shown in Fig. 3 here only evaluates whether the field-free switching of perpendicular magnetization is *allowed* by symmetry. It does not present information on the efficiency of such a switching behavior, or its underlying microscopic mechanisms, both of which may be different depending on the particular experimental implementation of the symmetry-breaking mechanism. The same is true in the cases of magnetic and chiral symmetry breaking discussed in the next sections, although in each case, we will point out relevant underlying mechanisms to the extent that they are known or can be hypothesized.

A first example of this approach is shown in Fig. 3c, where the lateral structural symmetry is broken by incorporating a film with varying thickness in the device[67]. This results in directional SOT-induced switching, where the directionality is determined by the lateral gradient of the interfacial anisotropy in the device. This mechanism, which was subsequently reproduced in structures with varying thickness of the oxide, ferromagnetic, and heavy metal layers[70,71], is surprisingly effective given that rather small thickness variations across an entire wafer can result in sizeable effective out-of-plane (field-like) SOT, which allows for directional switching in the presence of in-plane current. A second approach to break in-plane symmetry within an SOT-MRAM device was reported in[72], where the thickness variation is localized within each device, thus resulting in a tilted anisotropy axis.

While these studies convincingly demonstrated the role of broken in-plane symmetry in giving rise to directional SOT-MRAM switching, approaches based on structural symmetry-breaking are difficult to scale to large device numbers on an industry-relevant wafers size. As a result, more recent efforts have focused on breaking the *magnetic* in-plane symmetry of SOT-MRAM devices, without necessarily involving a structural asymmetry. Two examples of this (specifically, breaking mirror and chiral magnetic symmetries) are discussed in the next two sections.

VI. Field-free SOT-MRAM based on magnetic asymmetry

A possible approach to break the in-plane magnetic symmetry is the use of exchange bias (EB), by interfacing the ferromagnetic (FM) free layer in an SOT device with an appropriately chosen antiferromagnetic (AFM) film[73-75]. The exchange bias in such a system essentially replaces the external bias field, resulting in directional switching of the perpendicular magnetization. The AFM layer itself can serve as a source of SOT in this type of switching, though this is not necessarily required.

An example is illustrated in Fig. 4, which shows the deterministic switching of perpendicular magnetization in Co/Ni using SOT from an antiferromagnetic PtMn layer[73]. The directionality of switching clearly depends on the observed direction of the EB, consistent with the role of EB in breaking the in-plane symmetry in lieu of an external field.

Two challenges can be identified with this method: First, simultaneously achieving EB, large SOT efficiency, and sizeable perpendicular magnetic anisotropy (PMA) in the same material system is difficult and constrains the range of material options available for such devices. In particular, some of the most efficient generators of SOT reported to date, whether based on heavy metals or topological insulators[56,57,76], are not antiferromagnetic and may not promote PMA in adjacent layers. An interesting opportunity for such devices may be presented by the emergence of topological AFM materials in recent years, which exhibit AFM order while also having bulk or surface topological characteristics (i.e., Weyl or Dirac fermions)[77-81] that in turn may result in enhanced spin injection into adjacent ferromagnets. Importantly, some of these AFM materials have also been shown recently to be switchable by electric current themselves, e.g., using SOT from an adjacent heavy metal[82]. This means that if used as an SOT source, the directionality of their switching behavior could be programmed and reconfigured after device fabrication.

Second, the EB in most AFM/FM heterostructures studied to date is nonuniform, and depends on the local orientation of the Néel vector (i.e., the domain structure) within the AFM layer[83]. This makes it difficult to achieve uniform switching characteristics in devices whose size is small enough to be comparable to the typical AFM domain size, i.e., ~200 nm or less in most sputter-deposited AFM metals. On the other hand, achieving large domain size in AFM layers is significantly more difficult than in FM materials, due to the absence of the dominant magnetic dipole energy, which makes the Néel vector distribution much more susceptible to local crystal structure, grain size, defects, strain, and other parameters that are harder to control during material growth and subsequent processing. The progress in such AFM/FM heterostructure EB-SOT devices may, however, be accelerated by recent ongoing work – often motivated by using the AFM layer itself as the storage element[84-88] – to understand, image, model, and control domain structure in AFM films[89-92]. As pointed out later in Section IX, this EB nonuniformity may also be utilized in emerging designs for hardware security, which aim to exploit rather than suppress the device-to-device variations that result from it.

It is also worth noting that recent works have shown the promise of certain materials – including some AFM materials[93,94] – with reduced crystalline symmetries in generating unconventional SOT with a net perpendicular spin polarization, without the need for exchange bias. Effectively, these methods can be classified as breaking structural symmetry at the microscopic (rather than the device) level, and thereby can be a promising path towards SOT-MRAM devices if the underlying material properties can be reproduced with sufficient uniformity over a large wafer size. Recent perspectives and reviews have treated the progress in this area[95], so we will not focus on it in more detail within this paper.

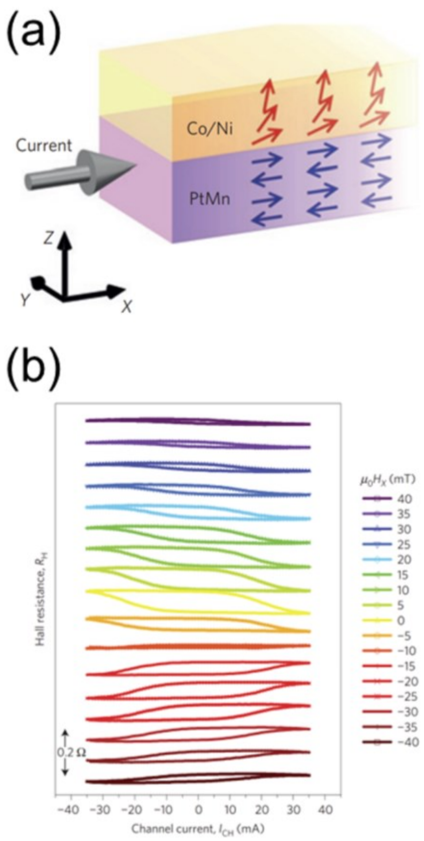

Fig. 4: Deterministic SOT switching of a perpendicular magnet using in-plane broken symmetry due to the exchange bias (EB) effect (Reproduced with permission from Ref. 73). (a) Schematic illustration of the EB-induced symmetry-breaking in a perpendicularly magnetized Co/Ni ferromagnetic layer interfaced with an antiferromagnetic PtMn film. (b) Current-induced switching loops measured using the anomalous Hall effect, demonstrating the deterministic current-induced switching in the absence of an external bias field (yellow curve).

VII. Field-free SOT-MRAM based on chiral asymmetry

The above-mentioned challenges of the EB approach have recently motivated efforts to realize directional switching in structures where chiral magnetic symmetry is broken within a single magnetic layer, which acts as the free layer of the device[96-98]. An example of this approach is shown in Fig. 5. Here, a CoTb layer was developed with a vertical composition gradient, where the ratio of Co and Tb within the amorphous ferrimagnetic layer was varied along the growth direction[98]. The combination of broken symmetry along the growth axis and large spin-orbit interaction within the CoTb layer resulted in a sizeable damping-like SOT, comparable in size to those achievable in heavy metal - ferromagnet bilayers. More interestingly, a Dzyaloshinskii-Moriya interaction (DMI) was also measured in these samples. Given that this DMI emerged from symmetry-breaking along the growth axis (perpendicular to the CoTb layer) due to the presence of the composition gradient, it exhibited the symmetry of an interfacial DMI. Unlike the latter, however, it extended within the bulk of the gradient film, and was thus referred to as a gradient-driven Dzyaloshinskii-Moriya interaction (gDMI).

The broken chiral symmetry of the sample due to gDMI resulted in a preferred direction of the perpendicular CoTb magnetization (which maintained a high PMA throughout the composition range studied) for a given direction of in-plane current in the sample. As a result, zero-field SOT-induced switching was achieved in these CoTb gradient samples, even though they did not exhibit any (non-magnetic) structural asymmetry within the plane.

Two additional experimental observations supported the hypothesis that gDMI is responsible for the field-free switching in these gradient samples. First, the sign of the SOT reversed for samples that had the opposite gradient direction along the growth axis, thus confirming that the self-torque originated from the broken symmetry due to this gradient. Second, the field required to eliminate the field-free SOT switching coincided with the gDMI field measured independently in the same samples (Fig. 5), confirming the role of gDMI in achieving the directional SOT switching.

Additional insights about the mechanism behind the switching were derived from investigating the role that the history of applied currents played in the device[98]. Specifically, it was shown that the SOT switching directionality is determined by the direction of the first in-plane write current applied to the device. Moreover, this "training" effect could be eliminated by applying a large magnetic field to the device to make it single-domain, after which the SOT switching directionality could be re-trained in the opposite direction by applying another training current. These observations are consistent with the presence of a current-induced chiral texture within the CoTb gradient sample, stabilized by the presence of gDMI. This may, in turn, result in a directional anisotropy similar to that previously observed in spin glass systems[99-103], which replaces the role of the external field and exchange bias in the previous two approaches.

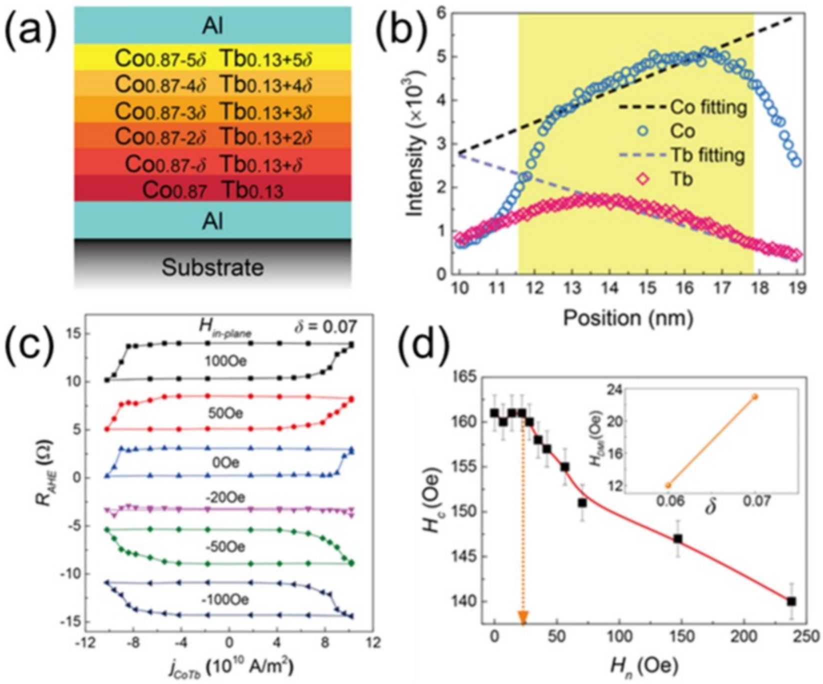

Fig. 5: Deterministic SOT switching of a perpendicular ferrimagnet using chiral symmetry-breaking due to a gradient-driven DMI (Reproduced with permission from Ref. 98). (a) Schematic and (b) energy dispersive x-ray spectroscopy (EDS) measured composition of a CoTb ferrimagnet with vertically varying ratio of Co and Tb. (c) The simultaneous presence of SOT and gradient-driven DMI in the film enables directional switching of the perpendicular magnetization using in-plane currents. (d) The experimentally measured DMI field corresponds well with the in-plane bias field required to destroy the directionality of the switching. The inset shows the dependence of the DMI field on the composition gradient δ, indicated in panel (a).

Compared to interfacial DMI[104], one of the potential advantages of using gDMI for deterministic SOT switching is that it extends throughout the bulk of a relatively thick magnetic film. Thus, the combination of SOT and gDMI can result in deterministic switching of substantially thicker (and therefore, more thermally stable) free layers[98].

It is also worth noting that the recently demonstrated interlayer DMI[105,106], which may be present between two ferromagnets coupled through a thin metallic spacer layer, can also result in chiral symmetry-breaking in layered magnetic structures. This type of DMI has indeed been demonstrated to result in both chiral textures and tilted anisotropy[107,108], and has recently been shown to also result in field-free SOT switching[109,110]. This represents another potential pathway towards field-free SOT-MRAM based on chiral asymmetry.

VIII. Towards practical field-free SOT-MRAM arrays

Translating the field-free switching approaches discussed above into practical SOT-MRAM device candidates suitable for integration into products entails several engineering challenges and open scientific questions. Here we outline a few of these, that we expect to provide fruitful avenues for fundamental and applied research in the near future.

- <u>Microscopic understanding of gDMI and its role in enabling directional switching:</u> The gDMI devices discussed in the previous section present open questions related to both their operating mechanism and materials engineering. First, the switching directionality of the devices is set (i.e., trained) by the first current pulse applied to them[98]. A better fundamental understanding of the microscopic mechanism of this training, which may originate from chiral magnetic textures within the CoTb layer, will be important to engineer practical devices. Second, the structure and size of such microscopic textures will affect the scalability of the switching mechanism. Therefore, a fruitful research direction involves imaging of such textures, determination of their micromagnetic structure, and their dependence on the history of applied currents. Third, the size of the gDMI can directly be enhanced by increasing the composition gradient slope, but this comes at the cost of a wider composition range for a given overall film thickness. Keeping the film perpendicular, on the other hand, is only possible within a range of Co to Tb ratios. Therefore, the writing efficiency may present a tradeoff against the magnetic anisotropy (hence thermal stability) of the device. A detailed investigation of this tradeoff and its dependence on the materials (including in other rare earth - transition metal combinations) is crucial to developing a strategy to engineer gDMI materials for SOT-MRAM applications.

- Switching speed: The SOT-switching can take place by uniform rotation of the magnetic state in single domain nanomagnets, or by the nucleation and movement of magnetic domain walls in micrometer-scale devices. These two dynamics present different speeds and relaxation time scales that can differ by orders of magnitude. As a result, the precise microscopic mechanism of symmetry breaking in SOT devices may have a significant effect on the achievable speed of writing information. Understanding the time-domain dynamics and fundamental speed limits of SOT-MRAM devices using the structural, magnetic, and chiral symmetry-breaking approaches described here will therefore be of increasing importance.
- Device variability: Minimizing device-to-device variations is a key requirement for a practical implementation of SOT devices in memory arrays. Breaking the SOT switching symmetry by the introduction of structural asymmetry (e.g., a thickness gradient as shown in Fig. 3) is therefore unlikely to lead to manufacturable solutions. In the case of the exchange bias mechanism, the natural magnetic and structural non-uniformities of the antiferromagnetic and ferromagnetic layers give rise to a distribution of exchange bias fields within a film, thus affecting the device-to-device variability, particularly for memory bits that are small enough to be comparable to the AFM grain size[83]. From this perspective, the gDMI-based chiral symmetry-breaking mechanism provides a potentially more scalable approach with lower device variations. Initial results, shown in Fig. 6, have indicated very uniform switching characteristics using this method across full 100 mm wafers based on CoTb gradient films[98].
- Integration of electrical readout mechanisms with deterministic SOT structures: In this perspective we have focused on the deterministic writing mechanism of SOT devices. For memory applications, reliable readout of information via magnetoresistive (MR) effects is

equally critical. The most common readout method used in SOT switching experiments to date is the anomalous Hall effect, which, however, is too small to be of practical interest in memory products. Practical readout of information in gDMI-based SOT structures will likely require an MTJ structure, similar to the widely used MgO-CoFeB MTJs used in ferromagnetic STT-MRAM today. While CoTb-based MTJs have been demonstrated before[111,112], this still presents a significant materials challenge since rare earth - transition metal ferrimagnets are more prone to chemically reacting with adjacent layers in the device when compared to CoFeB, and typically do not have sufficient tolerance against high-temperature annealing (~400˚C), which is required for back-end of line integration of MTJs on CMOS[113]. This may be a significant challenge for gDMI devices, specifically, since diffusion of atoms at higher processing temperatures may also make it harder to maintain a large composition gradient within the film.

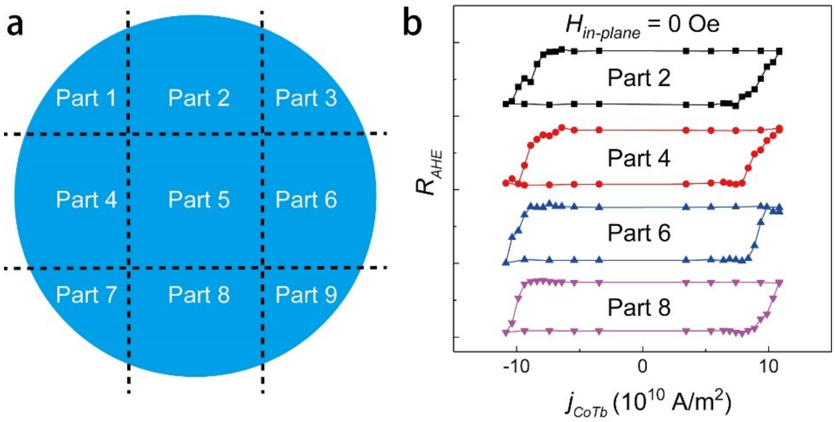

Fig. 6: SOT-induced switching using chiral symmetry-breaking shows uniform characteristics across a 100 mm wafer, as shown here based on switching data from Hall bars made from a CoTb film with a vertical composition gradient (Reproduced with permission from Ref. 98).

IX. Field-free SOT devices for unconventional computing and security applications

In addition to conventional applications as a memory cell, the increasing adoption of MRAM within the semiconductor industry provides unprecedented opportunities for innovation in computing architectures using the physics of nanomagnets[114-116]. Here, we briefly highlight two such opportunities taking advantage of field-free SOT-MRAM devices.

- <u>Computing with stochastic magnetic bits:</u> Nanoscale magnets are inherently stochastic elements. It is therefore possible to engineer MRAM-like devices where stochastic thermally-induced switching dominates the device behavior, in sharp contrast to memory applications where low bit error rates are required. Such "probabilistic" bits, which oscillate between their 0 and 1 states, can then be used to implement a range of new computing architectures[35,117,118]. When the energy barrier between the two free layer states in an MTJ is low enough, its resistance will oscillate between its low and high states under thermal fluctuations, effectively turning thermal noise into an electrical signal as a true random number generator (TRNG). The probability of finding 0s and 1s in a bitstream generated by the MTJ can in turn be tuned by applying an appropriate directional damping-like torque to it, e.g., using SOT in structures similar to those discussed in earlier sections. This results in a highly compact 1T-1R or 2T-1R MRAM cell operating as a TRNG, providing a significant energy and area reduction compared to existing CMOS-based pseudo random number generators that typically require thousands of transistors[31,119].

A stochastic computing artificial neural network (SC-ANN) implemented using such MTJ-based TRNGs (in this case, controlled by conventional STT) is shown in Fig. 7. In SC, decimal numbers are mapped to stochastic bitstreams, where the electrically tunable probability of finding 1s or 0s in the bitstream signifies a number in the range of -1 to 1[31]. This allows for the use of simple bit-wise logic gates for performing arithmetic operations, making multiplication- and addition-heavy ANNs smaller and more energy-efficient. An example is shown in Fig. 7, where an SC-ANN implemented using only six MTJs performs hand-written digit recognition, with an accuracy that depends on the length of the stochastic bitstreams used by the network[31].

Probabilistic bits can also be used to implement a different paradigm of computing where the memory cell itself (or more precisely, an appropriately interconnected network of probabilistic bits) "computes" the answer to a computational problem by naturally evolving to its lowest-energy state. Programming such a computer then involves mapping the computing problem onto this physical network, such as to allow the lowest-energy state of the network to be interpreted as the solution to the target problem. This method has been demonstrated to be highly efficient in solving optimization problems including integer factorization[119] and maximum satisfiability[34,36]. The proven scalability of MRAM within existing foundry manufacturing processes, as well as its room-temperature operation, make these types of probabilistic computers highly promising for emerging domain-specific computing chips.

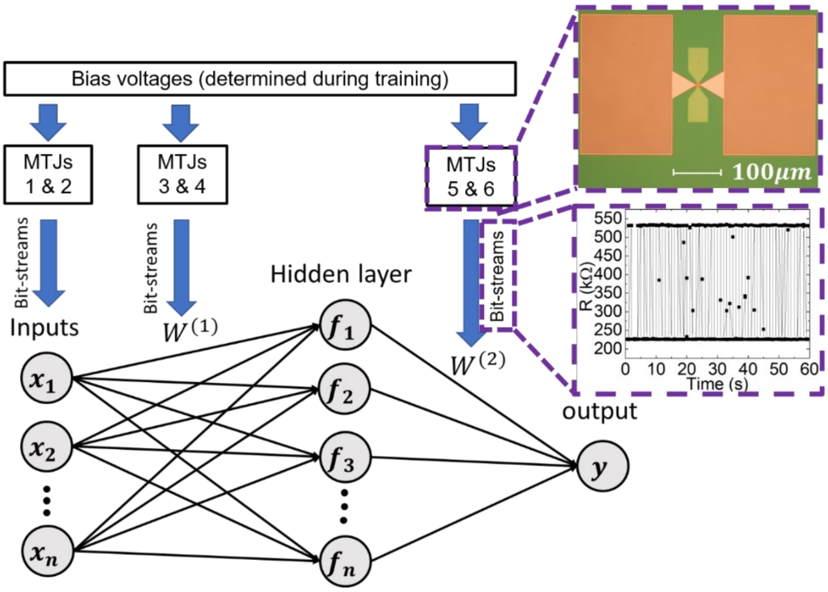

Fig. 7. Structure of an SC-ANN demonstrated using six stochastic MTJs to provide bit-streams for the inputs and weights in each layer of the network (Reproduced with permission from Ref. 31). The SC-ANN successfully performed hand-written digit recognition with an accuracy that is dynamically tunable by changing the bitstream length.

- Physically unclonable functions: Another opportunity for SOT-MRAM devices beyond conventional memory are security applications. Secure hardware building blocks such as physically unclonable functions (PUFs)[120,121] are gaining importance due to the supply chain challenges faced by the semiconductor industry, where trust in the hardware used for a specific product (using chips manufactured by an outside party) is not easily guaranteed. Recently, a number of PUF designs based on SOT devices have been proposed[122-127]. An example is illustrated in Fig. 8, where a PUF concept exploiting field-free SOT switching is demonstrated using an exchange-biased IrMn/CoFeB/Ta/CoFeB structure. Up to 15 instances are shown, which all meet the essential statistical properties of a PUF. Unlike an SOT-MRAM device where uniform exchange bias (thus resulting in a well-defined SOT switching directionality) is desired, in this experiment the exchange bias direction is randomized by annealing the structure under an oscillating magnetic field. Hence, the entropy source of this PUF is the stochasticity of the directional switching polarity of the perpendicular CoFeB layer, resulting from the random distribution of the exchange bias field at the IrMn/CoFeB interface.

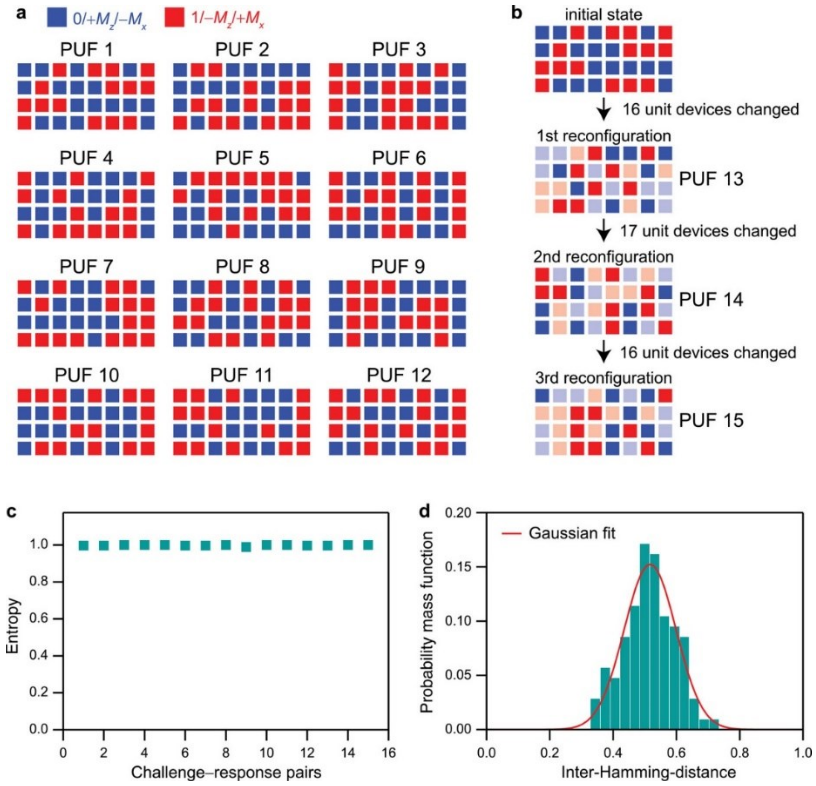

Fig. 8. Images and characterization of exchange-biased SOT PUFs (Reproduced with permission from Ref. 127). (a) 12 different spintronic PUF instances obtained using the same material structure. Red and blue squares indicate opposite SOT switching polarities. (b) Reconfiguration of PUFs using a field annealing process to randomize the exchange bias direction. (c) Entropy of 15 different spintronic PUFs. (d) Probability mass function versus inter-Hamming-distance of 15 different spintronic PUFs implemented using this approach.

X. Conclusions

Spin-orbit torques provide a pathway towards achieving a better combination of performance, density, and endurance in SOT-MRAM compared to existing STT-MRAM products. However, to operate with perpendicularly magnetized free layers, they require a structural, magnetic, or chiral in-plane symmetry-breaking mechanism. While examples of each type of symmetry-breaking have been demonstrated, challenges remain in terms of achieving a manufacturable and scalable method to realize deterministic field-free SOT-MRAM. Specifically, most magnetic and structural symmetry-breaking approaches to date have suffered from uniformity issues that may hinder their adoption, while chiral symmetry-breaking approaches still need more work to fundamentally understand their underlying physics, as well as their performance at short time scales. Regardless of the particular write mechanism used, integration with TMR readout is also required to enable high-density arrays. Beyond memory, the adoption of MRAM devices provides unique opportunities for architectural innovation in computing systems, with probabilistic computing and physically unclonable functions being two promising examples.

Acknowledgements

The authors acknowledge support by the National Science Foundation through award numbers 2203243, 1919109, 1853879, and by the National Science Foundation Materials Research Science and Engineering Center at Northwestern University (award number 1720319).

References

1 Gorton, I., Greenfield, P., Szalay, A. & Williams, R. Data-intensive computing in the 21st century. *Computer* **41**, 30-32 (2008).
2 Makarov, A., Sverdlov, V. & Selberherr, S. Emerging memory technologies: Trends, challenges, and modeling methods. *Microelectronics Reliability* **52**, 628-634 (2012).
3 Meena, J. S., Sze, S. M., Chand, U. & Tseng, T.-Y. Overview of emerging nonvolatile memory technologies. *Nanoscale research letters* **9**, 1-33 (2014).
4 Yu, S. & Chen, P.-Y. Emerging memory technologies: Recent trends and prospects. *IEEE Solid-State Circuits Magazine* **8**, 43-56 (2016).
5 Wang, K. L. & Amiri, P. K. Nonvolatile Spintronics: Perspectives on Instant-on Nonvolatile Nanoelectronic Systems. *SPIN* **02**, 1250009, doi:10.1142/s2010324712500099 (2012).
6 Golonzka, O. *et al.* in *2018 IEEE International Electron Devices Meeting (IEDM).* 18.11.11-18.11.14.
7 Ito, S. *et al.* in *2018 IEEE International Memory Workshop (IMW).* 1-4.
8 Kang, S. H. in *2014 Symposium on VLSI Technology (VLSI-Technology): Digest of Technical Papers.* 1-2.
9 Slaughter, J. M. *et al.* in *2016 IEEE International Electron Devices Meeting (IEDM)* 21.25.21-21.25.24 (2016).
10 Lin, C. S. *et al.* in *2020 IEEE Symposium on VLSI Technology.* 1-2.
11 Khan, F. *et al.* Design Optimization and Modeling of Charge Trap Transistors (CTTs) in 14 nm FinFET Technologies. *IEEE Electron Device Letters* **40**, 1100-1103,

doi:10.1109/LED.2019.2919871 (2019).
12 Yang, H. *et al.* Two-dimensional materials prospects for non-volatile spintronic memories. *Nature* **606**, 663-673, doi:10.1038/s41586-022-04768-0 (2022).
13 Gallagher, W. J. *et al.* in *2019 IEEE International Electron Devices Meeting (IEDM).* 2.7.1-2.7.4.
14 Fong, S. W., Neumann, C. M. & Wong, H. S. P. Phase-Change Memory—Towards a Storage-Class Memory. *IEEE Transactions on Electron Devices* **64**, 4374-4385, doi:10.1109/TED.2017.2746342 (2017).
15 Freitas, R. F. & Wilcke, W. W. Storage-class memory: The next storage system technology. *IBM Journal of Research and Development* **52**, 439-447, doi:10.1147/rd.524.0439 (2008).
16 Kim, T. & Lee, S. Evolution of Phase-Change Memory for the Storage-Class Memory and Beyond. *IEEE Transactions on Electron Devices* **67**, 1394-1406, doi:10.1109/TED.2020.2964640 (2020).
17 Wang, Z. *et al.* Postcycling Degradation in Metal-Oxide Bipolar Resistive Switching Memory. *IEEE Transactions on Electron Devices* **63**, 4279-4287, doi:10.1109/TED.2016.2604370 (2016).
18 Carboni, R. *et al.* in *2016 IEEE International Electron Devices Meeting (IEDM).* 21.26.21-21.26.24.
19 Sharma, D. D. in *2022 IEEE Symposium on High-Performance Interconnects (HOTI).* 5-12.
20 Sharma, D. D. in *2021 IEEE Symposium on High-Performance Interconnects (HOTI).* xii-xii.
21 Choi, S., Yang, J. & Wang, G. Emerging Memristive Artificial Synapses and Neurons for Energy-Efficient Neuromorphic Computing. *Advanced Materials* **32**, 2004659 (2020).
22 Guo, R., Lin, W., Yan, X., Venkatesan, T. & Chen, J. Ferroic tunnel junctions and their application in neuromorphic networks. *Applied Physics Reviews* **7**, 011304 (2020).
23 Li, Y., Wang, Z., Midya, R., Xia, Q. & Yang, J. J. Review of memristor devices in neuromorphic computing: materials sciences and device challenges. *Journal of Physics D: Applied Physics* **51**, 503002 (2018).
24 Zidan, M. A., Strachan, J. P. & Lu, W. D. The future of electronics based on memristive systems. *Nature electronics* **1**, 22-29 (2018).
25 Sangwan, V. K. & Hersam, M. C. Neuromorphic nanoelectronic materials. *Nature nanotechnology* **15**, 517-528 (2020).
26 Kim, K. *et al.* in *Proceedings of the 53rd Annual Design Automation Conference.* 1-6.
27 Li, J. *et al.* in *2017 22nd Asia and South Pacific Design Automation Conference (ASP-DAC).* 115-120 (IEEE).
28 Yu, G. *et al.* Room-Temperature Skyrmion Shift Device for Memory Application. *Nano Letters* **17**, 261-268, doi:10.1021/acs.nanolett.6b04010 (2017).
29 Li, Z. *et al.* HEIF: Highly efficient stochastic computing-based inference framework for deep neural networks. *IEEE Transactions on Computer-Aided Design of Integrated Circuits and Systems* **38**, 1543-1556 (2018).
30 Schott, M. *et al.* The Skyrmion Switch: Turning Magnetic Skyrmion Bubbles on and off with an Electric Field. *Nano Letters* **17**, 3006-3012, doi:10.1021/acs.nanolett.7b00328 (2017).
31 Shao, Y. *et al.* Implementation of Artificial Neural Networks Using Magnetoresistive Random-Access Memory-Based Stochastic Computing Units. *IEEE Magnetics Letters* **12**, 1-5, doi:10.1109/LMAG.2021.3071084 (2021).

32 Sim, H. & Lee, J. in *Proceedings of the 54th Annual Design Automation Conference 2017.* 1-6.
33 Finocchio, G. *et al.* The promise of spintronics for unconventional computing. *Journal of Magnetism and Magnetic Materials* **521**, 167506 (2021).
34 Aadit, N. A. *et al.* Massively parallel probabilistic computing with sparse Ising machines. *Nature Electronics*, 1-9 (2022).
35 Camsari, K. Y., Sutton, B. M. & Datta, S. P-bits for probabilistic spin logic. *Applied Physics Reviews* **6**, 011305 (2019).
36 Grimaldi, A. *et al.* Spintronics-compatible Approach to Solving Maximum-Satisfiability Problems with Probabilistic Computing, Invertible Logic, and Parallel Tempering. *Physical Review Applied* **17**, 024052 (2022).
37 Slonczewski, J. C. Conductance and exchange coupling of two ferromagnets separated by a tunneling barrier. *Physical Review B* **39**, 6995 (1989).
38 Tedrow, P. M. & Meservey, R. Spin-dependent tunneling into ferromagnetic nickel. *Physical Review Letters* **26**, 192 (1971).
39 Julliere, M. Tunneling between ferromagnetic films. *Physics letters A* **54**, 225-226 (1975).
40 Miyazaki, T. & Tezuka, N. Giant magnetic tunneling effect in Fe/Al2O3/Fe junction. *Journal of magnetism and magnetic materials* **139**, L231-L234 (1995).
41 Miyazaki, T. & Tezuka, N. Spin polarized tunneling in ferromagnet/insulator/ferromagnet junctions. *Journal of magnetism and magnetic materials* **151**, 403-410 (1995).
42 Moodera, J. S., Kinder, L. R., Wong, T. M. & Meservey, R. Large magnetoresistance at room temperature in ferromagnetic thin film tunnel junctions. *Physical review letters* **74**, 3273 (1995).
43 Yuasa, S., Nagahama, T., Fukushima, A., Suzuki, Y. & Ando, K. Giant room-temperature magnetoresistance in single-crystal Fe/MgO/Fe magnetic tunnel junctions. *Nature Materials* **3**, 868-871, doi:10.1038/nmat1257 (2004).
44 Parkin, S. S. P. *et al.* Giant tunnelling magnetoresistance at room temperature with MgO (100) tunnel barriers. *Nature Materials* **3**, 862-867, doi:10.1038/nmat1256 (2004).
45 Katine, J. A., Albert, F. J., Buhrman, R. A., Myers, E. B. & Ralph, D. C. Current-Driven Magnetization Reversal and Spin-Wave Excitations in Co/Cu/Co Pillars. *Physical Review Letters* **84**, 3149-3152, doi:10.1103/PhysRevLett.84.3149 (2000).
46 Katine, J. A. & Fullerton, E. E. Device implications of spin-transfer torques. *Journal of Magnetism and Magnetic Materials* **320**, 1217-1226, doi:https://doi.org/10.1016/j.jmmm.2007.12.013 (2008).
47 Mangin, S. *et al.* Current-induced magnetization reversal in nanopillars with perpendicular anisotropy. *Nature Materials* **5**, 210-215, doi:10.1038/nmat1595 (2006).
48 Slonczewski, J. C. Current-driven excitation of magnetic multilayers. *Journal of Magnetism and Magnetic Materials* **159**, L1-L7, doi:https://doi.org/10.1016/0304-8853(96)00062-5 (1996).
49 Huai, Y., Albert, F., Nguyen, P., Pakala, M. & Valet, T. Observation of spin-transfer switching in deep submicron-sized and low-resistance magnetic tunnel junctions. *Applied Physics Letters* **84**, 3118-3120, doi:10.1063/1.1707228 (2004).
50 Krizakova, V., Perumkunnil, M., Couet, S., Gambardella, P. & Garello, K. Spin-orbit torque switching of magnetic tunnel junctions for memory applications. *Journal of Magnetism and Magnetic Materials* **562**, 169692, doi:https://doi.org/10.1016/j.jmmm.2022.169692 (2022).

51 Gosavi, T. A. *et al.* Experimental Demonstration of Efficient Spin–Orbit Torque Switching of an MTJ With Sub-100 ns Pulses. *IEEE Transactions on Magnetics* **53**, 1-7, doi:10.1109/TMAG.2017.2707402 (2017).
52 Reza, A. K. & Roy, K. Topological semi-metal Na3Bi as efficient spin injector in current driven magnetic tunnel junction. *Journal of Applied Physics* **126**, 233901, doi:10.1063/1.5087077 (2019).
53 Miron, I. M. *et al.* Perpendicular switching of a single ferromagnetic layer induced by in-plane current injection. *Nature* **476**, 189-193, doi:10.1038/nature10309 (2011).
54 Liu, L., Lee, O. J., Gudmundsen, T. J., Ralph, D. C. & Buhrman, R. A. Current-Induced Switching of Perpendicularly Magnetized Magnetic Layers Using Spin Torque from the Spin Hall Effect. *Physical Review Letters* **109**, 096602, doi:10.1103/PhysRevLett.109.096602 (2012).
55 Liu, L. *et al.* Spin-Torque Switching with the Giant Spin Hall Effect of Tantalum. *Science* **336**, 555-558, doi:10.1126/science.1218197 (2012).
56 Mellnik, A. R. *et al.* Spin-transfer torque generated by a topological insulator. *Nature* **511**, 449-451, doi:10.1038/nature13534 (2014).
57 Fan, Y. *et al.* Magnetization switching through giant spin–orbit torque in a magnetically doped topological insulator heterostructure. *Nature Materials* **13**, 699-704, doi:10.1038/nmat3973 (2014).
58 Brataas, A. & Hals, K. M. D. Spin–orbit torques in action. *Nature Nanotechnology* **9**, 86-88, doi:10.1038/nnano.2014.8 (2014).
59 Zhang, C., Takeuchi, Y., Fukami, S. & Ohno, H. Field-free and sub-ns magnetization switching of magnetic tunnel junctions by combining spin-transfer torque and spin–orbit torque. *Applied Physics Letters* **118**, 092406, doi:10.1063/5.0039061 (2021).
60 Wang, M. *et al.* Field-free switching of a perpendicular magnetic tunnel junction through the interplay of spin–orbit and spin-transfer torques. *Nature Electronics* **1**, 582-588, doi:10.1038/s41928-018-0160-7 (2018).
61 Sato, N., Xue, F., White, R. M., Bi, C. & Wang, S. X. Two-terminal spin–orbit torque magnetoresistive random access memory. *Nature Electronics* **1**, 508-511, doi:10.1038/s41928-018-0131-z (2018).
62 Khalili Amiri, P. Spin torques join forces in a memory device. *Nature Electronics* **1**, 576-577, doi:10.1038/s41928-018-0164-3 (2018).
63 Ikeda, S. *et al.* A perpendicular-anisotropy CoFeB–MgO magnetic tunnel junction. *Nature Materials* **9**, 721-724, doi:10.1038/nmat2804 (2010).
64 Khalili Amiri, P. *et al.* Switching current reduction using perpendicular anisotropy in CoFeB–MgO magnetic tunnel junctions. *Applied Physics Letters* **98**, 112507, doi:10.1063/1.3567780 (2011).
65 Worledge, D. C. *et al.* Spin torque switching of perpendicular Ta|CoFeB|MgO-based magnetic tunnel junctions. *Applied Physics Letters* **98**, 022501, doi:10.1063/1.3536482 (2011).
66 Kong, W. J. *et al.* All-electrical manipulation of magnetization in magnetic tunnel junction via spin–orbit torque. *Applied Physics Letters* **116**, 162401, doi:10.1063/5.0001758 (2020).
67 Yu, G. *et al.* Switching of perpendicular magnetization by spin–orbit torques in the absence of external magnetic fields. *Nature Nanotechnology* **9**, 548-554, doi:10.1038/nnano.2014.94 (2014).

68 Şimşek, T. Field-Free Spin-Orbit Torque Switching in Magnetic Tunnel Junction Structures With Stray Fields. *IEEE Magnetics Letters* **12**, 1-5, doi:10.1109/LMAG.2021.3063081 (2021).

69 Fukami, S., Anekawa, T., Zhang, C. & Ohno, H. A spin–orbit torque switching scheme with collinear magnetic easy axis and current configuration. *Nature Nanotechnology* **11**, 621-625, doi:10.1038/nnano.2016.29 (2016).

70 Yu, G. *et al.* Current-driven perpendicular magnetization switching in Ta/CoFeB/[TaOx or MgO/TaOx] films with lateral structural asymmetry. *Applied Physics Letters* **105**, 102411, doi:10.1063/1.4895735 (2014).

71 Razavi, A. *et al.* Deterministic Spin–Orbit Torque Switching by a Light-Metal Insertion. *Nano Letters* **20**, 3703-3709, doi:10.1021/acs.nanolett.0c00647 (2020).

72 You, L. *et al.* Switching of perpendicularly polarized nanomagnets with spin orbit torque without an external magnetic field by engineering a tilted anisotropy. *Proceedings of the National Academy of Sciences* **112**, 10310, doi:10.1073/pnas.1507474112 (2015).

73 Fukami, S., Zhang, C., DuttaGupta, S., Kurenkov, A. & Ohno, H. Magnetization switching by spin–orbit torque in an antiferromagnet–ferromagnet bilayer system. *Nature Materials* **15**, 535-541, doi:10.1038/nmat4566 (2016).

74 Razavi, S. A. *et al.* Joule Heating Effect on Field-Free Magnetization Switching by Spin-Orbit Torque in Exchange-Biased Systems. *Physical Review Applied* **7**, 024023, doi:10.1103/PhysRevApplied.7.024023 (2017).

75 Peng, S. *et al.* Exchange bias switching in an antiferromagnet/ferromagnet bilayer driven by spin–orbit torque. *Nature Electronics* **3**, 757-764, doi:10.1038/s41928-020-00504-6 (2020).

76 Navabi, A. *et al.* Control of Spin-Wave Damping in YIG Using Spin Currents from Topological Insulators. *Physical Review Applied* **11**, 034046, doi:10.1103/PhysRevApplied.11.034046 (2019).

77 Deng, Y., Li, R. & Liu, X. Thickness dependent anomalous Hall effect in noncollinear antiferromagnetic Mn3Sn polycrystalline thin films. *Journal of Alloys and Compounds* **874**, 159910, doi:https://doi.org/10.1016/j.jallcom.2021.159910 (2021).

78 Khadka, D. *et al.* Kondo physics in antiferromagnetic Weyl semimetal Mn3+xSn1−x films. *Science Advances* **6**, eabc1977, doi:10.1126/sciadv.abc1977.

79 Nakatsuji, S., Kiyohara, N. & Higo, T. Large anomalous Hall effect in a non-collinear antiferromagnet at room temperature. *Nature* **527**, 212-215, doi:10.1038/nature15723 (2015).

80 Kuroda, K. *et al.* Evidence for magnetic Weyl fermions in a correlated metal. *Nature Materials* **16**, 1090-1095, doi:10.1038/nmat4987 (2017).

81 Ikhlas, M. *et al.* Large anomalous Nernst effect at room temperature in a chiral antiferromagnet. *Nature Physics* **13**, 1085-1090, doi:10.1038/nphys4181 (2017).

82 Tsai, H. *et al.* Electrical manipulation of a topological antiferromagnetic state. *Nature* **580**, 608-613, doi:10.1038/s41586-020-2211-2 (2020).

83 Kurenkov, A., Zhang, C., DuttaGupta, S., Fukami, S. & Ohno, H. Device-size dependence of field-free spin-orbit torque induced magnetization switching in antiferromagnet/ferromagnet structures. *Applied Physics Letters* **110**, 092410, doi:10.1063/1.4977838 (2017).

84 Arpaci, S. *et al.* Observation of current-induced switching in non-collinear antiferromagnetic IrMn3 by differential voltage measurements. *Nature Communications* **12**, 3828, doi:10.1038/s41467-021-24237-y (2021).

85 Shi, J. *et al.* Electrical manipulation of the magnetic order in antiferromagnetic PtMn pillars.

Nature Electronics **3**, 92-98, doi:10.1038/s41928-020-0367-2 (2020).

86 Wang, H. *et al.* Giant anisotropic magnetoresistance and nonvolatile memory in canted antiferromagnet Sr2IrO4. *Nature Communications* **10**, 2280, doi:10.1038/s41467-019-10299-6 (2019).

87 Feng, Z., Yan, H. & Liu, Z. Electric-Field Control of Magnetic Order: From FeRh to Topological Antiferromagnetic Spintronics. *Advanced Electronic Materials* **5**, 1800466, doi:https://doi.org/10.1002/aelm.201800466 (2019).

88 Wadley, P. *et al.* Electrical switching of an antiferromagnet. *Science* **351**, 587-590, doi:10.1126/science.aab1031 (2016).

89 Grzybowski, M. J. *et al.* Imaging Current-Induced Switching of Antiferromagnetic Domains in CuMnAs. *Physical Review Letters* **118**, 057701, doi:10.1103/PhysRevLett.118.057701 (2017).

90 Sapozhnik, A. A. *et al.* Direct imaging of antiferromagnetic domains in ${\mathrm{Mn}}_{2}\mathrm{Au}$ manipulated by high magnetic fields. *Physical Review B* **97**, 134429, doi:10.1103/PhysRevB.97.134429 (2018).

91 Xu, J. *et al.* Imaging antiferromagnetic domains in nickel oxide thin films by optical birefringence effect. *Physical Review B* **100**, 134413, doi:10.1103/PhysRevB.100.134413 (2019).

92 Tomasello, R. *et al.* Domain periodicity in an easy-plane antiferromagnet with Dzyaloshinskii-Moriya interaction. *Physical Review B* **102**, 224432, doi:10.1103/PhysRevB.102.224432 (2020).

93 Bose, A. *et al.* Tilted spin current generated by the collinear antiferromagnet ruthenium dioxide. *Nature Electronics* **5**, 267-274, doi:10.1038/s41928-022-00744-8 (2022).

94 Zhang, W. *et al.* Giant facet-dependent spin-orbit torque and spin Hall conductivity in the triangular antiferromagnet IrMn3. *Science Advances* **2**, e1600759, doi:10.1126/sciadv.1600759 (2016).

95 Sklenar, J. *et al.* Perspective: Interface generation of spin-orbit torques. *Journal of Applied Physics* **120**, 180901, doi:10.1063/1.4967391 (2016).

96 Wu, H. *et al.* Chiral Symmetry Breaking for Deterministic Switching of Perpendicular Magnetization by Spin–Orbit Torque. *Nano Letters* **21**, 515-521, doi:10.1021/acs.nanolett.0c03972 (2021).

97 Sloika, M. I., Kravchuk, V. P., Sheka, D. D. & Gaididei, Y. Curvature induced chirality symmetry breaking in vortex core switching phenomena. *Applied Physics Letters* **104**, 252403, doi:10.1063/1.4884957 (2014).

98 Zheng, Z. *et al.* Field-free spin-orbit torque-induced switching of perpendicular magnetization in a ferrimagnetic layer with a vertical composition gradient. *Nature Communications* **12**, 4555, doi:10.1038/s41467-021-24854-7 (2021).

99 Fert, A. & Levy, P. M. Role of Anisotropic Exchange Interactions in Determining the Properties of Spin-Glasses. *Physical Review Letters* **44**, 1538-1541, doi:10.1103/PhysRevLett.44.1538 (1980).

100 Levy, P. M. & Fert, A. Anisotropy induced by nonmagnetic impurities in Cu Mn spin-glass alloys. *Physical Review B* **23**, 4667-4690, doi:10.1103/PhysRevB.23.4667 (1981).

101 Hippert, F., Alloul, H. & Fert, A. Anisotropy energy of CuMn spin glasses. *Journal of Applied Physics* **53**, 7702-7704, doi:10.1063/1.330143 (1982).

102 Fert, A. & Hippert, F. Anisotropy of Spin-Glasses from Torque Measurements. *Physical Review*

Letters **49**, 1508-1511, doi:10.1103/PhysRevLett.49.1508 (1982).

103 Fert, A., Arvanitis, D. & Hippert, F. Triad anisotropy of spin glasses and torque experiments (invited). *Journal of Applied Physics* **55**, 1640-1645, doi:10.1063/1.333428 (1984).

104 Ma, X. *et al.* Interfacial control of Dzyaloshinskii-Moriya interaction in heavy metal/ferromagnetic metal thin film heterostructures. *Physical Review B* **94**, 180408, doi:10.1103/PhysRevB.94.180408 (2016).

105 Fernández-Pacheco, A. *et al.* Symmetry-breaking interlayer Dzyaloshinskii–Moriya interactions in synthetic antiferromagnets. *Nature Materials* **18**, 679-684, doi:10.1038/s41563-019-0386-4 (2019).

106 Han, D.-S. *et al.* Long-range chiral exchange interaction in synthetic antiferromagnets. *Nature Materials* **18**, 703-708, doi:10.1038/s41563-019-0370-z (2019).

107 Avci, C. O., Lambert, C.-H., Sala, G. & Gambardella, P. Chiral Coupling between Magnetic Layers with Orthogonal Magnetization. *Physical Review Letters* **127**, 167202, doi:10.1103/PhysRevLett.127.167202 (2021).

108 Kim, H.-J. *et al.* Field-Free Switching of Magnetization by Tilting the Perpendicular Magnetic Anisotropy of Gd/Co Multilayers. *Advanced Functional Materials* **32**, 2112561, doi:https://doi.org/10.1002/adfm.202112561 (2022).

109 Huang, Y.-H., Huang, C.-C., Liao, W.-B., Chen, T.-Y. & Pai, C.-F. Growth-Dependent Interlayer Chiral Exchange and Field-Free Switching. *Physical Review Applied* **18**, 034046, doi:10.1103/PhysRevApplied.18.034046 (2022).

110 He, W. *et al.* Field-Free Spin–Orbit Torque Switching Enabled by the Interlayer Dzyaloshinskii–Moriya Interaction. *Nano Letters* **22**, 6857-6865, doi:10.1021/acs.nanolett.1c04786 (2022).

111 Chen, T.-J. *et al.* The magnetic characteristics of perpendicular magnetic tunnel junction with MgO and Al–O oxidation layers in various thickness. *Journal of Magnetism and Magnetic Materials* **304**, e291-e293, doi:https://doi.org/10.1016/j.jmmm.2006.02.108 (2006).

112 Nishimura, N. *et al.* Magnetic tunnel junction device with perpendicular magnetization films for high-density magnetic random access memory. *Journal of Applied Physics* **91**, 5246-5249, doi:10.1063/1.1459605 (2002).

113 Shao, Y. *et al.* Sub-volt switching of nanoscale voltage-controlled perpendicular magnetic tunnel junctions. *Communications Materials* **3**, 87, doi:10.1038/s43246-022-00310-x (2022).

114 Finocchio, G. *et al.* The promise of spintronics for unconventional computing. *Journal of Magnetism and Magnetic Materials* **521**, 167506, doi:https://doi.org/10.1016/j.jmmm.2020.167506 (2021).

115 Misra, S. *et al.* Probabilistic Neural Computing with Stochastic Devices. *Advanced Materials* **n/a**, 2204569, doi:https://doi.org/10.1002/adma.202204569 (2022).

116 Jung, S. *et al.* A crossbar array of magnetoresistive memory devices for in-memory computing. *Nature* **601**, 211-216, doi:10.1038/s41586-021-04196-6 (2022).

117 Camsari, K. Y., Faria, R., Sutton, B. M. & Datta, S. Stochastic p-bits for invertible logic. *Physical Review X* **7**, 031014 (2017).

118 Camsari, K. Y., Salahuddin, S. & Datta, S. Implementing p-bits with embedded MTJ. *IEEE Electron Device Letters* **38**, 1767-1770 (2017).

119 Borders, W. A. *et al.* Integer factorization using stochastic magnetic tunnel junctions. *Nature* **573**, 390-393 (2019).

120 Herder, C., Yu, M.-D., Koushanfar, F. & Devadas, S. Physical unclonable functions and applications: A tutorial. *Proceedings of the IEEE* **102**, 1126-1141 (2014).
121 Gao, Y., Al-Sarawi, S. F. & Abbott, D. Physical unclonable functions. *Nature Electronics* **3**, 81-91 (2020).
122 Finocchio, G. *et al.* Spin–orbit torque based physical unclonable function. *Journal of Applied Physics* **128**, 033904 (2020).
123 Puliafito, V. *et al.* Impact of Scaling on Physical Unclonable Function Based on Spin–Orbit Torque. *IEEE Magnetics Letters* **11**, 1-5 (2020).
124 Zhang, J. *et al.* Spin–orbit torque-based reconfigurable physically unclonable functions. *Applied Physics Letters* **116**, 192406 (2020).
125 Zhang, S. *et al.* Reconfigurable physical unclonable cryptographic primitives based on current-induced nanomagnets switching. *Science China Information Sciences* **65**, 1-9 (2022).
126 Divyanshu, D., Kumar, R., Khan, D., Amara, S. & Massoud, Y. Physically Unclonable Function using GSHE driven SOT assisted p-MTJ for next generation hardware security applications. *IEEE Access* **10**, 93029-93038 (2022).
127 Lee, S. *et al.* Spintronic Physical Unclonable Functions Based on Field-free Spin-orbit Torque Switching. *Advanced Materials*, 2203558 (2022).